





Article

Tofacitinib Blocks Enteseal Lymphocyte Activation and Modulates MSC Adipogenesis, but Does Not Directly Affect Chondro- and Osteogenesis

Tobias Russell ^{1,*}, Hannah Rowe ^{1,*}, Charlie Bridgewood ¹, Richard J. Cuthbert ¹, Abdulla Watad ^{1,2}, Darren Newton ³, Elena Jones ¹ and Dennis McGonagle ¹

- ¹ Leeds Institute of Rheumatic and Musculoskeletal Medicine (LIRMM), University of Leeds, Leeds LS9 7TF, UK; medcbri@leeds.ac.uk (C.B.); r.j.cuthbert@leeds.ac.uk (R.J.C.); watad.abdulla@gmail.com (A.W.); e.jones@leeds.ac.uk (E.J.); meddgm@leeds.ac.uk (D.M.)
- ² Department of Medicine B and Zabludowicz Center for Autoimmune Diseases, Sheba Medical Center, Tel-Hashomer, Ramat-Gan, Israel, Sackler Faculty of Medicine, Tel-Aviv University, Tel-Aviv 69978, Israel
- ³ Division of Hematology and Immunology, Leeds Institute of Medical Research at St. James's, University of Leeds, Leeds LS9 7TF, UK; bmbdjn@leeds.ac.uk
- * Correspondence: umtjwr@leeds.ac.uk (T.R.); umhmr@leeds.ac.uk (H.R.)

Abstract: Enteseal spinal inflammation and new bone formation with progressive ankylosis may occur in ankylosing spondylitis (AS) and psoriatic arthritis (PsA). This study evaluated whether JAK inhibition with tofacitinib modulated the key disease associated cytokines, TNF and IL-17A, and whether tofacitinib also modulated bone marrow stromal cell-derived mesenchymal stem cell (MSCs) function, including osteogenesis, since post inflammation new bone formation occurs under these conditions. **Methods:** Conventional enteseal derived $\alpha\beta$ CD4+ and CD8+ T-cells were investigated following anti-CD3/CD28 bead stimulation to determine IL-17A and TNF levels in tofacitinib treated (1000 nM) peri-enteseal bone (PEB) and peripheral blood mononuclear cells (PBMC) using ELISA. Bone marrow stromal cell-derived mesenchymal stem cell (MSC) colony forming units (CFU-F) and multi-lineage potential were evaluated using tofacitinib (dosages ranging between 100, 500, 1000 and 10,000 nM). **Results:** Induced IL-17A and TNF cytokine production from both enteseal CD4+ T-cells and CD8+ T-cells was effectively inhibited by tofacitinib. Tofacitinib treatment did not impact on CFU-F potential or in vitro chondro- and osteogenesis. However, tofacitinib stimulation increased MSC adipogenic potential with greater Oil Red O stained areas. **Conclusion:** Inducible IL-17A and TNF production by healthy human enteseal CD4+ and CD8+ T-cells was robustly inhibited in vitro by tofacitinib. However, tofacitinib did not impact MSC osteogenesis, but stimulated in vitro MSC adipogenesis, the relevance of which needs further evaluation given that the adipocytes are associated with new bone formation in SpA.

Keywords: tofacitinib; JAK-STAT; ankylosing spondylitis



Citation: Russell, T.; Rowe, H.; Bridgewood, C.; Cuthbert, R.J.; Watad, A.; Newton, D.; Jones, E.; McGonagle, D. Tofacitinib Blocks Enteseal Lymphocyte Activation and Modulates MSC Adipogenesis, but Does Not Directly Affect Chondro- and Osteogenesis. *Immuno* **2021**, *1*, 545–557. <https://doi.org/10.3390/immuno1040038>

Academic Editor: Ulrich Sack

Received: 8 October 2021

Accepted: 26 November 2021

Published: 2 December 2021

Publisher's Note: MDPI stays neutral with regard to jurisdictional claims in published maps and institutional affiliations.



Copyright: © 2021 by the authors. Licensee MDPI, Basel, Switzerland. This article is an open access article distributed under the terms and conditions of the Creative Commons Attribution (CC BY) license (<https://creativecommons.org/licenses/by/4.0/>).

1. Introduction

The seronegative spondyloarthropathies (SpA) encompass Ankylosing Spondylitis (AS), its non-radiographic predecessor and PsA (Psoriatic Arthritis), including peripheral and axial disease. Cytokines including TNF and IL-17A are pivotal in the pathogenesis of the seronegative SpA in both experimental settings and, more importantly, in humans, as demonstrated by the success of cytokine targeting [1]. A peculiar aspect of successful anti-TNF therapy in well-established AS was progressive new bone formation over the following years [2]. Likewise, in experimental SpA models, short-term control of inflammation failed to stop the progress of ankylose [3].

Skeletal tissue repair and remodeling responses are orchestrated by tissue-resident stromal cells, including mesenchymal stem cells (MSCs) which have been identified in the synovium, periosteum, bone marrow and synovial fluid [4–8] and have been reported at

the entheses, which are the target sites of new bone formation in AS [9,10]. MSCs have been closely studied due to their ability to differentiate into numerous lineages including osteocytes, chondrocytes and adipocytes [11]. In recent years, it has been established that animal models of SpA have resident immune cell populations at the enthesis and, in particular, immune cells that produce abundant IL-17A [12,13], where this cytokine can modulate aberrant bone formation reactions. The human enthesis also contains both innate and adaptive immune cell populations that are capable of producing TNF and IL-17A, such as Gamma Delta, CD4+ and CD8+ T-cells [13,14]. Animal models of SpA, as well as showing new bone formation, also show decreased bone marrow adipose tissue (BMAT) [15].

The JAK kinase inhibitors have emerged as important targets in the SpA group of diseases [16], and it is interesting that neither TNF nor IL-17A signal directly through the JAK pathways. Tofacitinib is a highly selective Janus kinase (JAK)-1 and JAK3 and also, to a lesser extent, tyrosine kinase 2 (TYK2) inhibitor, licensed for rheumatoid arthritis (RA) [17–19] and PsA [20]. Tofacitinib is a competitive inhibitor, and binds to the adenosine triphosphate (ATP) binding site in the catalytic cleft of the kinase domain of JAK. Tofacitinib serves to mimic the structure of ATP, but is missing the triphosphate group; thus, tofacitinib inhibits phosphorylation and JAK activation, and in turn the phosphorylation and activation of STAT. This results in decreased transcription and decreased production of cytokines [21].

JAKs are integral to a number of cytokine and growth factor signaling cascades [22] that may affect TNF and IL-17A production indirectly. The use of JAKs is expanding in the SpA arena, and efficacy is as good as the anti-TNF agents [23]. It has previously been shown that tofacitinib inhibits T-cell derived IL-17A, but not previously at the enthesis [24].

Given the observation that new bone formation in AS may continue despite suppression of inflammation, an impact of JAK inhibition on MSC differentiation could be on tissue repair and new bone formation. For example, in vitro, tofacitinib treatment inhibited bone-marrow derived fibroblasts' differentiation into myofibroblasts [25]. A recent study showed that tofacitinib augmented human MSC osteogenesis that was noted to be relevant for bone erosion in RA [26]. In the context of joint disease, the treatment of osteoarthritic MSCs with tofacitinib during chondrogenic differentiation in vitro suggested that it could, in part, rescue the reduction in glycosaminoglycan content [27]. Hence, JAK inhibition could theoretically affect stromal tissue responses in the joint organ in different chronic joint diseases, in addition to its impact on immune cells.

In this study, we evaluated the in vitro effects of tofacitinib on tissue responses in the enthesis, including its impact on enthesal lymphocyte activation and MSC function. In an in vitro enthesitis model, we showed that it robustly suppressed conventional $\alpha\beta$ CD4+ T-cell activation and attenuated enthesal derived IL-17A and TNF production. Our data suggest that tofacitinib had no direct effects on in vitro marrow MSC osteogenesis but that it stimulated adipogenesis, the latter observation being of interest given the role of fat in axial new bone formation in SpA [28].

2. Materials and Methods

2.1. Patient Consent and Collection of Samples

Written informed consent was given by all patients, and research was carried out in compliance with the Helsinki Declaration. Ethics committee approval was obtained from the Leeds East Ethics Committee under permit number 06/Q1206/127. Bone marrow (BM) aspirates were taken from the iliac crest of patients with acute trauma or patients undergoing elective orthopaedic surgery [29]. Enthesal sample collection was approved by the North West-Greater Manchester West Research Ethics Committee (REC: 16/NW/0797).

2.2. Isolation of Primary Cells from Enthesis and Matched Blood

Enthesal samples were separated into enthesal soft tissue (EST) and peri-enthesal bone (PEB), and both were enzymatically digested as previously described [12]. For both

cell preparations, blood and enthesal cells, density gradient separation (Lymphoprep, Stemcell Technology, Cambridge, UK) was conducted to obtain peripheral blood mononuclear cells (PBMCs) and enthesal mononuclear cells (EMCs), respectively, using methods previously described [30].

2.3. Magnetic Cell Separation

Following the isolation of EMCs from digested enthesal samples and also of PBMCs from processed blood, CD4+ and CD8+ T-cells were subsequently isolated using biotinylated anti-CD4 or CD8 antibodies (both from Miltenyi Biotech, Bergisch Gladbach, Germany). Cells were isolated using magnetic separation (Miltenyi Biotech LS columns), according to the manufacturer's instructions.

2.4. Cell Preparation

Following cell isolation, CD4+ and CD8+ T-cells were plated out in a 96-well plate (minimum of 5×10^4 cells/well) in RPMI (GIBCO, Waltham, MA, USA) containing 10% fetal calf serum (FCS) and 1% penicillin/streptomycin.

For inhibition studies, cells were incubated with tofacitinib 1000 nM (Pfizer) and DMSO control (0.1%). Tofacitinib was diluted to maintain a final concentration of 0.1% DMSO. Cells were stimulated using anti-CD3/CD28 (GIBCO) for 48 h.

2.5. TNF and IL-17A Determination by ELISA in Enthesal Stimulated Cell Supernatants

Following 48 h stimulation, cells were removed by centrifugation and the supernatant was frozen and stored at -80 °C. Concentrations of TNF and IL-17A were quantified using sandwich ELISAs from eBioscience/ThermoFisher (Waltham, MA, USA). ELISAs were carried out according to the manufacturer's protocol. Following this, pg/mL and pg/cell were calculated.

2.6. CFU-F Assay and Measurement of Colony Area

The CFU-F assay performed was a modification of the method described by Galotto et al. [31]. BM aspirate (100 μ L) was seeded, in duplicate, in 100 mm diameter tissue culture dishes in StemMACS media (Miltenyi Biotech). Tofacitinib was added in concentrations of 100 nM, 500 nM, 1000 nM and 10,000 nM. Alternatively, dimethyl sulfoxide (DMSO) was used as a carrier control and an unstimulated control was also included. Assessment of colony number and measurement of colony size then proceeded as previously described [29].

2.7. In Vitro Osteogenesis, Chondrogenesis and Adipogenesis

Following the removal of erythrocytes, BM aspirates were seeded at a density of 8×10^4 cells/cm² into tissue culture grade flasks (Corning, New York, NY, USA) with StemMACS media and incubated in standard culture conditions (5% CO₂, 37 °C). Adherent cells were expanded to <80% confluence, then passaged, re-seeded at 4.5×10^3 cells/cm² and returned to culture; up to three passages were performed. Osteogenic differentiation and assessment of alkaline phosphatase (ALP) activity, as well as matrix mineralization by measurement of calcium accumulation, was measured as previously described [32,33] at 14 and 21 days after initiation of osteogenic conditions, respectively. Calcium was extracted by incubation with 600 mM hydrochloric acid for 4 h at 4 °C. Calcium levels were measured using a Calcium Liquid Colorimetric Assay Kit (Sentinel Diagnostics, Milan, Italy). Osteogenic differentiation media was supplemented with 500, 1000 or 10,000 nM tofacitinib or carrier control, DMSO. For assessment of chondrogenesis, cell pellets were incubated in chondrogenic conditions for 21 days and glycosaminoglycan (GAG) accumulation was visualized histologically as well as measured quantitatively, as previously described [32,33], using the Blyscan™ Glycosaminoglycan Assay (Bicolor). Adipogenic differentiation was performed over 14 days and visualized by oil red staining, as previously described [32,33]; photomicrographs were captured using a CKX41 inverted light

microscope and analyzed using image analysis software NIS elements (Nikon). Adipogenic differentiation and quantitative measurement was performed over 14 days using Nile red fluorescence and measured using a Mithras LB940 luminescent plate reader (Berthold), as previously described [34]. In all cases, the differentiation media was supplemented with 500 nM, 1000 nM or 10,000 nM tofacitinib or DMSO carrier control.

To further explore the effect of tofacitinib on adipogenesis, adipogenic differentiation was repeated over a period of 21 days and concentrations of 10 nM, 50 nM, 100 nM and 500 nM, as well as a DMSO control, were added to the differentiation media.

2.8. Statistics

For the *in vitro* datasets, the Shapiro–Wilk normality test was used to assess distribution normality and to determine appropriate correlation and significance testing. For datasets which contained fewer than six data points per group, a non-Gaussian distribution was assumed. Statistical significance is defined as $p < 0.05$: * indicates $p < 0.05$, ** indicates $p < 0.01$, *** indicates $p < 0.001$. All statistics were calculated using SPSS[®] Version 25 or GraphPad Prism. Graphs were generated using GraphPad Prism[®] Version 8.01. For the *in vitro* experiments, box and whisker plots show median (line) interquartile range (box) and extreme values (whiskers). Error bars represent the standard error of the mean (SEM); refer to the results section for specific tests used per experimental procedure.

3. Results

3.1. Effect of Tofacitinib on Bone Marrow MSC CFU-F Potential

We evaluated the colony-forming properties of the bone marrow cells after low-density plating using standard assays. Tofacitinib had no effect on bone marrow MSC CFU-F potential, overall colony area or the average size of individual colonies at any of the concentrations tested (Figure 1A–C).

3.2. The Effect of Tofacitinib on *In Vitro* MSC Trilineage Differentiation

To study whether tofacitinib affects the multi-lineage potential of MSCs, we studied its effect in osteogenic, chondrogenic and adipogenic differentiation assays. Treatment during osteogenic induction of MSCs had no noticeable effect on alkaline phosphatase (ALP) activity after 14 days of differentiation (Figure 1D), and the accumulation of calcium was similarly unaffected (Figure 1E). We also evaluated the effect of tofacitinib on cartilage differentiation. Again, treatment with the JAK inhibitor did not induce a difference in the accumulation of GAGs, pellet formation or GAG content in chondrogenic pellet cultures (Figure 1F). This was further confirmed with quantitative measurement of GAG production (Figure 1G).

Tofacitinib treatment dose-dependently increased MSC adipogenesis as measured by oil red staining at day 14 (Figure 2A). The median proportion of the area occupied by lipid vacuoles in the control was measured at 5.43%, which increased significantly to 9.32% and 11.76% in the 1000 nM and 10,000 nM ($n = 6$, $p < 0.05$) tofacitinib treatment, respectively (Figure 2B), following paired *t*-tests. These data suggest that JAK inhibition by tofacitinib in MSCs leads to an increase in adipogenesis.

3.3. Increased Adipogenesis Is Linked to Cell Proliferation

To obtain better insights into the effects of tofacitinib on adipogenesis, we further evaluated the differentiation cultures. Significantly increased fat formation was also shown with Nile red staining (Figure 3A) with a 2.29-fold increase ($n = 6$, $p < 0.05$) in median fluorescence emission with 10,000 nM tofacitinib treatment, following Dunn's post-hoc testing (Figure 3B). Using lower concentrations of tofacitinib for 21 days showed a clear dose-dependent increase in fat formation (Figure 3C). A significant increase in Nile red fluorescence was seen for 100nM ($n = 7$, $p < 0.05$; 1.36-fold) and 500 nM ($n = 7$, $p < 0.0005$; 2.10-fold) tofacitinib treatment relative to the control, following Dunn's post-hoc testing.

We then studied whether tofacitinib affects in vitro pre-adipocyte proliferation and subsequent fat accumulation [35]. Firstly, induction of adipogenesis resulted in a significant increase in DAPI fluorescence reflecting cell numbers compared to the control at day 14, for all tofacitinib concentrations (500 nM; 1.44-fold, 1000 nM; 1.40 and 10,000 nM; 1.69-fold. $p = 0.028$), but with the biggest increase at the lowest 500 nM dose (Figure 3D). A day 21 DAPI signal was significantly increased compared to the control in all samples (50 nM; 1.07-fold, 100 nM; 1.05-fold and 500 nM; 1.10-fold $p < 0.05$ for all concentrations) (Figure 3E) except 10 nM treatment. Together with colony-forming assays, in which no increases in undifferentiated MSC proliferation were found (Figure 3B), these data suggest that tofacitinib has a positive effect on the proliferation of pre-adipocytes, even in low concentrations.

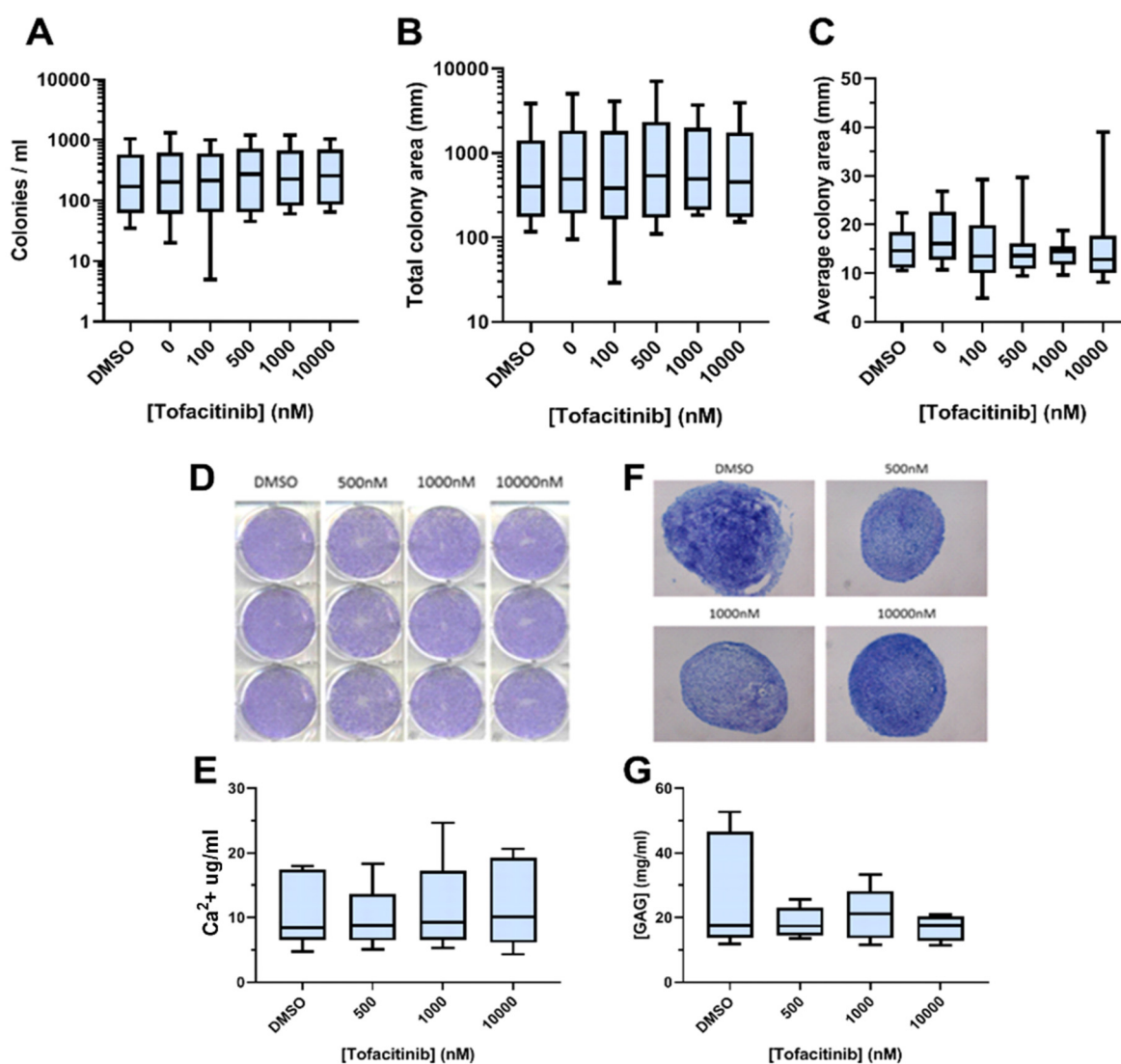


Figure 1. Tofacitinib does not affect MSC colony-forming potential, osteogenesis or chondrogenesis. (A) The effect of tofacitinib on the ability of BM MSCs to initiate adherent colonies and expand in vitro. (B) The effect of tofacitinib on the rate of MSC expansion measured as the total area occupied by colonies, or (C) as the mean area occupied by a single colony. Fast blue staining for ALP activity following osteogenic induction of MSC differentiation in the presence or absence of tofacitinib. Figure shows a single representative donor sample at day 14, in triplicate (D). The effect of tofacitinib on osteogenic differentiation assessed by accumulation of calcium at day 21 (E). The effect of tofacitinib on MSC chondrogenic differentiation, assessed by accumulation of GAGs at day 21. Toluidine blue staining of chondrogenic pellets (F). Quantitative assessment of GAG content in digested chondrogenic pellets (G).

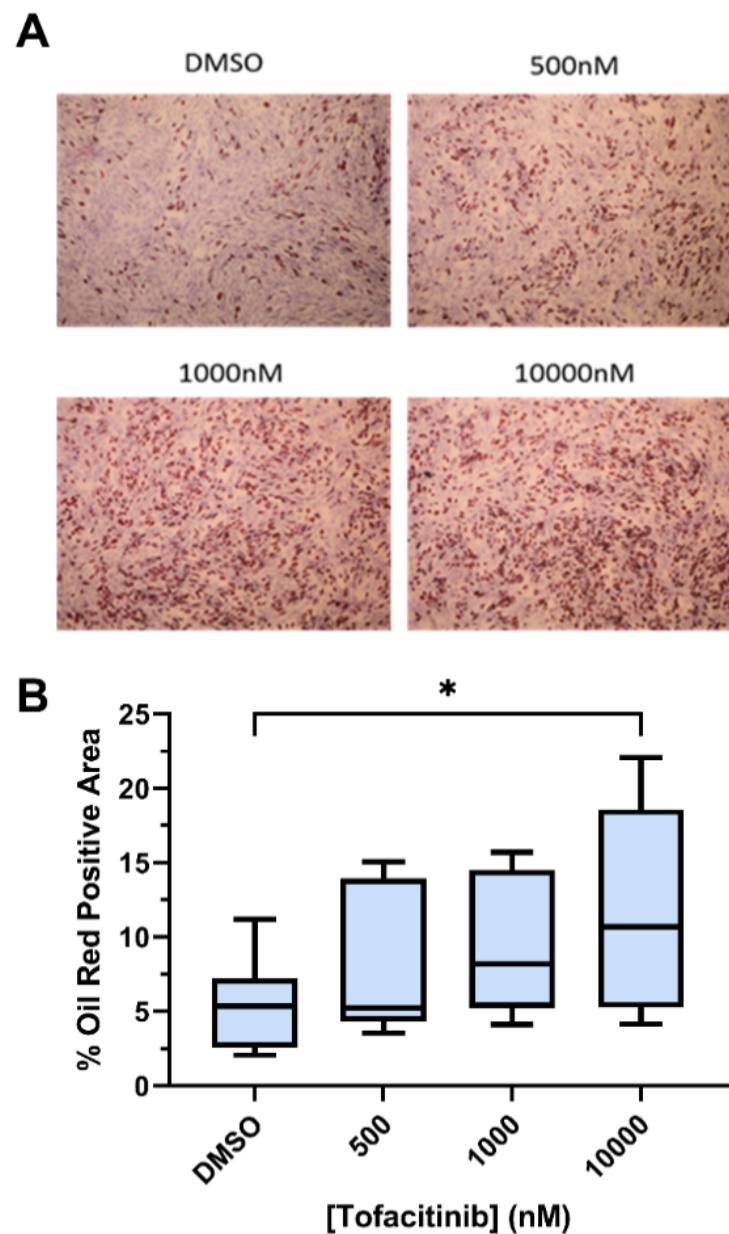


Figure 2. Tofacitinib stimulates adipogenesis of MSCs. Representative image showing the effect of tofacitinib treatment on adipogenesis, visualised with the uptake of oil red into lipid vacuoles (red) counterstained with haematoxylin (A). Measurement of oil red stained area of adipogenic cultures at day 14 (B). The median proportion of the area occupied by lipid vacuoles in the control was measured at 5.43%, which increased to 11.76% in the 10,000 nM ($n = 6$) tofacitinib treatment. Paired t -tests. $* = p < 0.05$.

3.4. Tofacitinib Inhibits Pro-Inflammatory Cytokine Production in an In Vitro Enthesitis Model

Following the selection of T-cells via magnetic separation, we assessed whether tofacitinib [1000 nM] had any impact on pro-inflammatory cytokine production, specifically IL-17A and TNF production by ELISA. Following stimulation, tofacitinib [1000 nM] effectively inhibited CD4+ and CD8+ T-cell IL-17A and TNF production, with the latter showing the most effective inhibition of cytokine production when treated with tofacitinib (Figure 4).

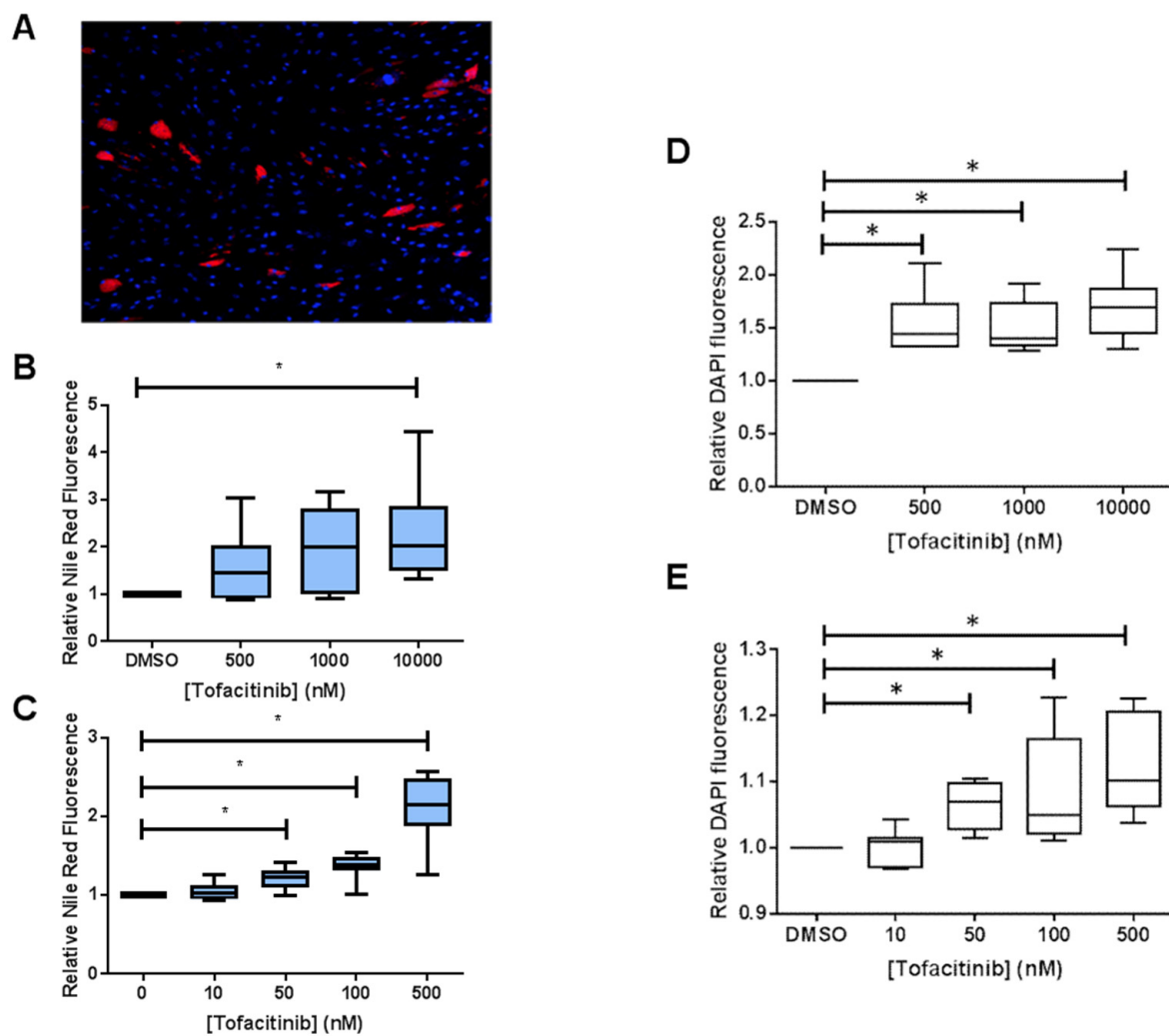


Figure 3. Adipogenic differentiation of MSCs measured by Nile red fluorescence. Representative image showing Nile red uptake into lipid vacuoles (red), counterstained with DAPI (blue) (A). Quantification of Nile red staining at day 14 with high tofacitinib dose (B) 2.29 ($n = 6$) fold increase in median fluorescence emission with 10,000 nM tofacitinib treatment and day 21 with lower tofacitinib treatment dose (C) significance seen in 100 ($n = 7$) and 500 nM ($n = 7$) tofacitinib treatment relative to the control following Dunn's post-hoc testing. Adipocyte hyperplasia during adipogenic differentiation in the presence of tofacitinib. Relative cell number measured by DAPI fluorescence at day 14 (D) (500 nM; 1.44-fold, 1000 nM; 1.40 and 10,000 nM; 1.69-fold) and day 21 (E) (50 nM; 1.07-fold, 100 nM; 1.05-fold and 500 nM; 1.10-fold). * = $p < 0.05$.

IL-17A production after CD3/CD28 stimulation of CD4+ T-cells isolated from PBMC was significantly inhibited by tofacitinib treatment ($n = 11$, $p < 0.01$, Figure 4A); this inhibition was also seen in CD4+ T-cells isolated from the PEB ($n = 12$, $p < 0.01$, Figure 1A). However, no significant inhibition was seen from the CD8+ T-cell populations at either the PEB or PBMC. CD4+ T-cells from PEB ($n = 12$, $p < 0.01$) and PBMC ($n = 11$, $p < 0.01$) showed significant reductions in TNF secretion after tofacitinib treatment (Figure 4B), with CD8+ T-cells from both PEB ($n = 12$, $p < 0.01$) and PBMC ($n = 11$, $p < 0.01$) showing similar reductions in TNF secretion. Ranges for all TNF and IL-17 values can be seen in Table 1.

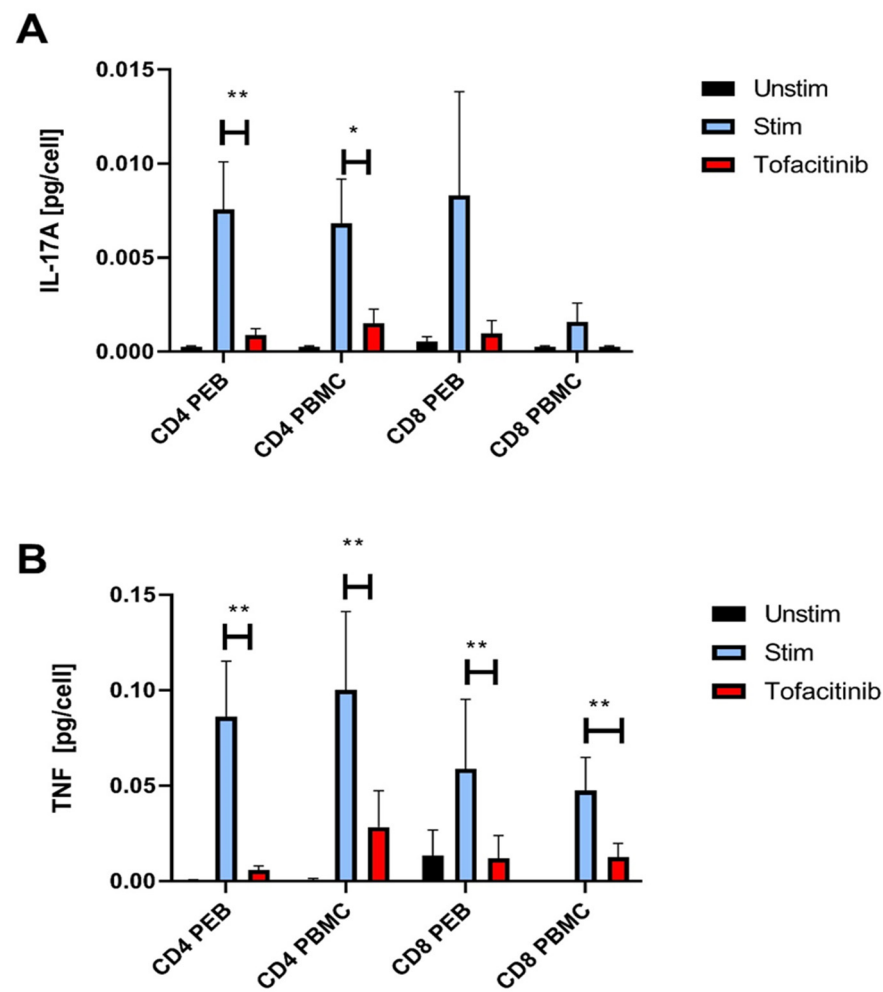


Figure 4. Tofacitinib inhibits pro-inflammatory cytokine production in an in vitro enthesitis model. Following isolation of enthesial CD4+ or CD8+ T-cells, cells were stimulated with anti-CD3/CD28 for 48 h with and without 1000 nM tofacitinib. IL-17A (A) and TNF (B), secretion was quantified by ELISA with post-hoc Wilcoxon signed rank testing. CD4+ T-cell from PEB ($n = 12$) and PBMC ($n = 11$) showed significant reductions in IL-17A secretion after tofacitinib treatment when stimulated. All cell populations tested CD4+ T-cells PEB ($n = 12$), PBMC ($n = 11$), CD8+ T-cells PEB ($n = 12$) and PBMC ($n = 11$) all showed significant reductions in TNF secretion induced by tofacitinib treatment after stimulation. * = $p < 0.05$, ** = $p < 0.01$.

Table 1. Mean \pm Standard Deviation of pg/cell values of TNF and IL-17 from CD4 PEB, CD4 PBMC, CD8 PEB and CD8 PBMC.

TNF pg/Cell	CD4 PEB	CD4 PBMC	CD8 PEB	CD8 PBMC
Unstimulated	0.0004221 \pm 0.001165	0.001223 \pm 0.002708	0.01347 \pm 0.0463	0.0001662 \pm 0.0003335
Stimulated	0.001165 \pm 0.1011	0.1719 \pm 0.1841	0.05894 \pm 0.1258	0.04349 \pm 0.05426
Tofacitinib	0.005911 \pm 0.007506	0.03026 \pm 0.06246	0.01205 \pm 0.04102	0.01268 \pm 0.02394
IL-17A pg/Cell	CD4 PEB	CD4 PBMC	CD8 PEB	CD8 PBMC
Unstimulated	0.0002852 \pm 0.0001011	0.0002733 \pm 0.0001464	0.0005429 \pm 0.0009168	0.0002722 \pm 0.000147
Stimulated	0.007574 \pm 0.008783	0.006828 \pm 0.007784	0.008313 \pm 0.01912	0.00159 \pm 0.003283
Tofacitinib	0.0008929 \pm 0.001153	0.001518 \pm 0.002472	0.0009734 \pm 0.002405	0.0002722 \pm 0.000147

4. Discussion

Adaptive immune cells present at the normal enthesis produce cytokines, including TNF and IL-17A, that are known to modify MSC function [36]. Accordingly, this work investigated the effect of tofacitinib, a JAK inhibitor, on the differentiation capacity of MSCs and on conventional $\alpha\beta$ CD4+ and CD8+ T-cells in an in vitro enthesitis model and its effect on bone marrow MSCs. Tofacitinib completely blocked IL-17A and TNF protein production from CD4+ T-cells in an in vitro enthesitis model. No effect was shown for MSC differentiation in osteogenic or chondrogenic conditions, but tofacitinib did increase MSC adipogenic differentiation.

In adipogenic conditions, tofacitinib concentrations as low as 50 nM were able to significantly increase the lipid content and cellularity of MSCs undergoing in vitro adipogenic differentiation. This is surprising, given that studies examining adipogenesis in 3T3-L1 cells, a widely used model for adipogenic differentiation [37–39], suggested that STAT5A and STAT5B activation promoted adipogenesis, particularly in the early stages of differentiation, and it could be expected that a JAK inhibitor would antagonise this process [38,40]. Additionally, JAK1-STAT3 activation has been implicated in the increased proliferation of pre-adipocytes before terminal differentiation [37,41]. However, pre-adipocytes are responsive to several cytokines that have been shown to inhibit adipogenesis, including IFN- γ [42], oncostatin M (OSM) [43] and neuropoietin [44], all of which are potent activators of JAK kinases and could suggest an explanation for the results detailed here. However, another hormone/cytokine that may explain our results is leptin, which has been identified in bone marrow derived mesenchymal precursors [45] culminating in adipogenesis and inhibition of osteogenic differentiation; interestingly, pre-adipocytes from the bone marrow are leptin receptor positive (LepR⁺), which signals through JAK2/STAT3 [46].

Further data have shown that adipose-specific disruption of JAK2 and STAT3 signaling in vivo results in increased adipose mass associated with hypertrophy and increased lipid content [47,48]. No such data appear available for JAK1 and JAK3, the preferred targets of tofacitinib. Shi et al. found that adipocyte-specific JAK2 deficiency led to impaired lipolysis with aging, suggesting that JAK2 inhibition may cause excessive lipid accumulation in mature adipocytes [48]. This is interesting, since hyperlipidemia has been reported as a side effect of tofacitinib treatment in patients with rheumatoid arthritis [18,19]. Further investigation is needed to elucidate the mechanism by which tofacitinib induces adipogenesis, with respect to signaling pathways.

The ability of tofacitinib to induce adipogenesis in vitro may also have important implications for in vivo osteogenesis and chondrogenesis. The limited in vivo effect may also be understood in this context, with JAK1/3 antagonism having an indirect impact on chondro- and osteogenesis. With increased expression of the master transcription factor for adipogenesis PPAR γ , this suppresses the activation of the master transcription factor for osteogenesis RUNX2 [49]. The lineage commitment towards adipogenesis requires significantly more DNA histone modification, decreasing osteogenic and chondrogenic differentiations which share an initial differentiation pathway [50].

With regards to the conventional $\alpha\beta$ T-cells, the results support the idea that these enthesial T-cells can secrete pivotal disease-relevant cytokines such as TNF and IL-17A following CD3/CD28 stimulation, without the use of other exogenous cytokines such as IL-23, where in vitro tofacitinib treatment inhibits this production. These results have been reported in other studies, showing an effective blockade of IL-17A production following tofacitinib therapy [51]. Through murine models and, also, clinical observations, both TNF and IL-17A have been heavily implicated in enthesitis-related pathology [52–54]. Whilst innate lymphocytes are major inflammatory cytokine producers in mice [55], these findings also suggest that conventional T-cell populations that can express these cytokines are present at the normal enthesis. Given the MHC-I and -II associations with human SpA spectrum disorders, the findings presented here highlight the importance of the investigation of enthesial T-cells in pathological conditions such as AS and PsA. This

in vitro system may provide a model for testing the impact of JAK/STAT inhibitors on the adaptive immune system in pre-clinical work in SpA.

IL-17A production has been extensively studied, and can either be produced dependently or independently of IL-23 signalling, where the latter involves unconventional innate-like T-cells including MAIT cells (mucosal associated invariant T), $\gamma\delta$ T cells, type 3 ILC'S (innate lymphoid cells) and iNKT (invariant natural killer T) cells [56–58]. The SKG mouse model, which carries a point mutation in the gene encoding the T cell receptor (TCR)-proximal signaling molecule ZAP-70, develops a T-cell-mediated autoimmune arthritis, which clinically and immunologically resembles SpA in humans [59]. It has been reported in previous studies utilising the SKG model that JAK inhibitors, including tofacitinib, are effective at reducing pro-inflammatory cytokine production (IL-17A) and increasing immunomodulatory cytokines (IL-10) [60–62], where the major arthritogenic T-cell subset within the SKG model, Th17, had its differentiation inhibited by tofacitinib [60]. Interestingly, the alternative isoform of the Th17 transcription factor, ROR γ , has been identified as a negative regulator of adipocyte differentiation when mediated by MMP3 (matrix metalloproteinase 3) in both mice and humans [63]. Due to significant sequence and functional similarities, the ROR subtypes co-expressed in cells may exhibit functional overlap [64].

5. Conclusions

In summary, JAK inhibition has directly inhibited CD4+ T-cell induced IL-17A and TNF production, and also MSC relevant transcript inhibition. No impact on MSC osteogenesis was noted, but it remains possible that indirect bone effects could occur via the adipogenic pathway. This suggests that clinical trials with JAK/STAT inhibitors in axial SpA should be carefully analyzed for effects concerning adipogenesis, as indirectly measured by fatty corner lesions on spinal MRI.

Author Contributions: T.R., H.R., R.J.C., A.W. and C.B. conducted experiments and wrote the manuscript. E.J., D.M., C.B. and D.N. contributed to experimental planning and critical discussion of results obtained, as well as manuscript correction. All authors have read and agreed to the published version of the manuscript.

Funding: D.M. is funded by the Leeds NIHR Biomedical Research Centre. Funding: Novartis UK investigator-initiated non-clinical research funding support (H.R., T.R. and C.B.), and research funded by a Pfizer investigator-initiated research grant (R.C.). A.W. was funded by the Celgene supported PARTNER fellowship program.

Institutional Review Board Statement: The study was conducted according to the guidelines of the Declaration of Helsinki and approved by the University of Leeds ethical approval committee. REC: 16/NW/0797.

Informed Consent Statement: Informed consent was obtained from all subjects involved in the study.

Acknowledgments: This article/paper/report presents independent research funded/supported by the National Institute for Health Research (NIHR) Leeds Biomedical Research Centre (BRC). The views expressed are those of the author(s) and not necessarily those of the NIHR or the Department of Health and Social Care Funding. The authors have declared no conflicts of interest. RJC is supported by a Pfizer investigator initiated research grant. DM is funded by the Leeds NIHR Biomedical Research Centre, Novartis UK investigator-initiated non-clinical research funding support (CB, TR, HR). AW was funded by the Celgene supported PARTNER fellowship program.

Conflicts of Interest: The authors declare no conflict of interest.

References

1. Bridgwood, C.; Watad, A.; Cuthbert, R.J.; McGonagle, D. Spondyloarthritis: New insights into clinical aspects, translational immunology and therapeutics. *Curr. Opin. Rheumatol.* **2018**, *30*, 526–532. [[CrossRef](#)]
2. Baraliakos, X.; Haibel, H.; Listing, J.; Sieper, J.; Braun, J. Continuous long-term anti-tnf therapy does not lead to an increase in the rate of new bone formation over 8 years in patients with ankylosing spondylitis. *Ann. Rheum. Dis.* **2014**, *73*, 710–715. [[CrossRef](#)] [[PubMed](#)]

3. Lories, R.J.; Derese, I.; de Bari, C.; Luyten, F.P. Evidence for uncoupling of inflammation and joint remodeling in a mouse model of spondylarthritis. *Arthritis Rheum.* **2007**, *56*, 489–497. [[CrossRef](#)]
4. De Bari, C.; Dell'Accio, F.; Tylzanowski, P.; Luyten, F.P. Multipotent mesenchymal stem cells from adult human synovial membrane. *Arthritis Rheum.* **2001**, *44*, 1928–1942. [[CrossRef](#)]
5. De Bari, C.; Dell'Accio, F.; Luyten, F.P. Human periosteum-derived cells maintain phenotypic stability and chondrogenic potential throughout expansion regardless of donor age. *Arthritis Rheum.* **2001**, *44*, 85–95. [[CrossRef](#)]
6. English, A.; Jones, E.A.; Corscadden, D.; Henshaw, K.; Chapman, T.; Emery, P.; McGonagle, D. A comparative assessment of cartilage and joint fat pad as a potential source of cells for autologous therapy development in knee osteoarthritis. *Rheumatology* **2007**, *46*, 1676–1683. [[CrossRef](#)]
7. Jones, E.A.; Crawford, A.; English, A.; Henshaw, K.; Mundy, J.; Corscadden, D.; Chapman, T.; Emery, P.; Hatton, P.; McGonagle, D. Synovial fluid mesenchymal stem cells in health and early osteoarthritis: Detection and functional evaluation at the single-cell level. *Arthritis Rheum.* **2008**, *58*, 1731–1740. [[CrossRef](#)]
8. Jones, E.; Churchman, S.M.; English, A.; Buch, M.H.; Horner, E.A.; Burgoyne, C.H.; Reece, R.; Kinsey, S.; Emery, P.; McGonagle, D.; et al. Mesenchymal stem cells in rheumatoid synovium: Enumeration and functional assessment in relation to synovial inflammation level. *Ann. Rheum. Dis.* **2010**, *69*, 450–457. [[CrossRef](#)] [[PubMed](#)]
9. Lories, R.J.; Derese, I.; Luyten, F.P. Modulation of bone morphogenetic protein signaling inhibits the onset and progression of ankylosing enthesitis. *J. Clin. Investig.* **2005**, *115*, 1571–1579. [[CrossRef](#)]
10. Schett, G.; Lories, R.J.; D'Agostino, M.-A.; Elewaut, D.; Kirkham, B.; Soriano, E.R.; McGonagle, D. Enthesitis: From pathophysiology to treatment. *Nat. Rev. Rheumatol.* **2017**, *13*, 731. [[CrossRef](#)] [[PubMed](#)]
11. Pittenger, M.F.; Discher, D.E.; Péault, B.M.; Phinney, D.G.; Hare, J.M.; Caplan, A.I. Mesenchymal stem cell perspective: Cell biology to clinical progress. *NPJ Regen. Med.* **2019**, *4*, 22. [[CrossRef](#)]
12. Cuthbert, R.J.; Fragkakis, E.M.; Dunsmuir, R.; Li, Z.; Coles, M.; Marzo-Ortega, H.; Giannoudis, P.V.; Jones, E.; El-Sherbiny, Y.M.; McGonagle, D. Brief report: Group 3 innate lymphoid cells in human enthesis. *Arthritis Rheumatol.* **2017**, *69*, 1816–1822. [[CrossRef](#)]
13. Cuthbert, R.J.; Watad, A.; Fragkakis, E.M.; Dunsmuir, R.; Loughenbury, P.; Khan, A.; Millner, P.A.; Davison, A.; Marzo-Ortega, H.; Newton, D.; et al. Evidence that tissue resident human enthesis gammadeltat-cells can produce il-17a independently of il-23r transcript expression. *Ann. Rheum. Dis.* **2019**, *78*, 1559–1565. [[CrossRef](#)]
14. Watad, A.; Rowe, H.; Russell, T.; Zhou, Q.; Anderson, L.K.; Khan, A.; Dunsmuir, R.; Loughenbury, P.; Borse, V.; Rao, A.; et al. Normal human enthesis harbours conventional cd4+ and cd8+ t cells with regulatory features and inducible il-17a and tnfr expression. *Ann. Rheum. Dis.* **2020**, *79*, 1044–1054. [[CrossRef](#)]
15. Furesi, G.; Fert, I.; Beaufrère, M.; Araujo, L.M.; Glatigny, S.; Baschant, U.; von Bonin, M.; Hofbauer, L.C.; Horwood, N.J.; Breban, M.; et al. Rodent models of spondyloarthritis have decreased white and bone marrow adipose tissue depots. *Front. Immunol.* **2021**, *12*, 665208. [[CrossRef](#)]
16. Veale, D.J.; McGonagle, D.; McInnes, I.B.; Krueger, J.G.; Ritchlin, C.T.; Elewaut, D.; Kanik, K.S.; Hendrikx, T.; Berstein, G.; Hodge, J. The rationale for janus kinase inhibitors for the treatment of spondyloarthritis. *Rheumatology* **2019**, *58*, 197–205. [[CrossRef](#)]
17. Burmester, G.R.; Blanco, R.; Charles-Schoeman, C.; Wollenhaupt, J.; Zerbini, C.; Benda, B.; Gruben, D.; Wallenstein, G.; Krishnaswami, S.; Zwillich, S.H.; et al. Tofacitinib (cp-690,550) in combination with methotrexate in patients with active rheumatoid arthritis with an inadequate response to tumour necrosis factor inhibitors: A randomised phase 3 trial. *Lancet* **2013**, *381*, 451–460. [[CrossRef](#)]
18. Van Vollenhoven, R.F.; Fleischmann, R.; Cohen, S.; Lee, E.B.; Garcia Mejjide, J.A.; Wagner, S.; Forejtova, S.; Zwillich, S.H.; Gruben, D.; Koncz, T.; et al. Tofacitinib or adalimumab versus placebo in rheumatoid arthritis. *N. Engl. J. Med.* **2012**, *367*, 508–519. [[CrossRef](#)]
19. Fleischmann, R.; Kremer, J.; Cush, J.; Schulze-Koops, H.; Connell, C.A.; Bradley, J.D.; Gruben, D.; Wallenstein, G.V.; Zwillich, S.H.; Kanik, K.S.; et al. Placebo-controlled trial of tofacitinib monotherapy in rheumatoid arthritis. *N. Engl. J. Med.* **2012**, *367*, 495–507. [[CrossRef](#)]
20. Gao, W.; McGarry, T.; Orr, C.; McCormick, J.; Veale, D.J.; Fearon, U. Tofacitinib regulates synovial inflammation in psoriatic arthritis, inhibiting stat activation and induction of negative feedback inhibitors. *Ann. Rheum. Dis.* **2016**, *75*, 311–315. [[CrossRef](#)]
21. Hodge, J.A.; Kawabata, T.T.; Krishnaswami, S.; Clark, J.D.; Telliez, J.-B.; Dowty, M.E.; Menon, S.; Lamba, M.; Zwillich, S. The mechanism of action of tofacitinib—an oral janus kinase inhibitor for the treatment of rheumatoid arthritis. *Clin. Exp. Rheumatol.* **2016**, *34*, 318–328.
22. O'Shea, J.J.; Schwartz, D.M.; Villarino, A.V.; Gadina, M.; McInnes, I.B.; Laurence, A. The jak-stat pathway: Impact on human disease and therapeutic intervention. *Annu. Rev. Med.* **2015**, *66*, 311–328. [[CrossRef](#)]
23. Charles-Schoeman, C.; Burmester, G.; Nash, P.; Zerbini, C.A.; Soma, K.; Kwok, K.; Hendrikx, T.; Bananis, E.; Fleischmann, R. Efficacy and safety of tofacitinib following inadequate response to conventional synthetic or biological disease-modifying antirheumatic drugs. *Ann. Rheum. Dis.* **2016**, *75*, 1293–1301. [[CrossRef](#)]
24. Maeshima, K.; Yamaoka, K.; Kubo, S.; Nakano, K.; Iwata, S.; Saito, K.; Ohishi, M.; Miyahara, H.; Tanaka, S.; Ishii, K. The jak inhibitor tofacitinib regulates synovitis through inhibition of interferon- γ and interleukin-17 production by human cd4+ t cells. *Arthritis Rheum.* **2012**, *64*, 1790–1798. [[CrossRef](#)]
25. Yan, J.; Zhang, Z.; Yang, J.; Mitch, W.E.; Wang, Y. Jak3/stat6 stimulates bone marrow-derived fibroblast activation in renal fibrosis. *J. Am. Soc. Nephrol. JASN* **2015**, *26*, 3060–3071. [[CrossRef](#)]

26. Gaber, T.; Brinkman, A.C.K.; Pienczikowski, J.; Diesing, K.; Damerau, A.; Pfeiffenberger, M.; Lang, A.; Ohrndorf, S.; Burmester, G.R.; Buttgerit, F.; et al. Impact of janus kinase inhibition with tofacitinib on fundamental processes of bone healing. *Int. J. Mol. Sci.* **2020**, *21*, 865. [[CrossRef](#)]
27. Van Beuningen, H.M.; de Vries-van Melle, M.L.; Vitters, E.L.; Schreurs, W.; van den Berg, W.B.; van Osch, G.J.; van der Kraan, P.M. Inhibition of tak1 and/or jak can rescue impaired chondrogenic differentiation of human mesenchymal stem cells in osteoarthritic-like conditions. *Tissue Eng. Part A* **2014**, *20*, 2243–2252. [[CrossRef](#)]
28. Baraliakos, X.; Boehm, H.; Bahrami, R.; Samir, A.; Schett, G.; Lubner, M.; Ramming, A.; Braun, J. What constitutes the fat signal detected by mri in the spine of patients with ankylosing spondylitis? A prospective study based on biopsies obtained during planned spinal osteotomy to correct hyperkyphosis or spinal stenosis. *Ann. Rheum. Dis.* **2019**, *78*, 1220–1225. [[CrossRef](#)]
29. Cuthbert, R.; Boxall, S.A.; Tan, H.B.; Giannoudis, P.V.; McGonagle, D.; Jones, E. Single-platform quality control assay to quantify multipotential stromal cells in bone marrow aspirates prior to bulk manufacture or direct therapeutic use. *Cytotherapy* **2012**, *14*, 431–440. [[CrossRef](#)]
30. Bridgewood, C.; Russell, T.; Weedon, H.; Baboolal, T.; Watad, A.; Sharif, K.; Cuthbert, R.; Wittmann, M.; Wechalekar, M.; McGonagle, D. The novel cytokine metrn1/il-41 is elevated in psoriatic arthritis synovium and inducible from both enthesal and synovial fibroblasts. *Clin. Immunol.* **2019**, *208*, 108253. [[CrossRef](#)]
31. Galotto, M.; Berisso, G.; Delfino, L.; Podesta, M.; Ottaggio, L.; Dallorso, S.; Dufour, C.; Ferrara, G.B.; Abbondandolo, A.; Dini, G.; et al. Stromal damage as consequence of high-dose chemo/radiotherapy in bone marrow transplant recipients. *Exp. Hematol.* **1999**, *27*, 1460–1466. [[CrossRef](#)]
32. Jones, E.; English, A.; Churchman, S.M.; Kouroupis, D.; Boxall, S.A.; Kinsey, S.; Giannoudis, P.G.; Emery, P.; McGonagle, D. Large-scale extraction and characterization of cd271+ multipotential stromal cells from trabecular bone in health and osteoarthritis: Implications for bone regeneration strategies based on uncultured or minimally cultured multipotential stromal cells. *Arthritis Rheum.* **2010**, *62*, 1944–1954.
33. Jones, E.A.; Kinsey, S.E.; English, A.; Jones, R.A.; Straszynski, L.; Meredith, D.M.; Markham, A.F.; Jack, A.; Emery, P.; McGonagle, D. Isolation and characterization of bone marrow multipotential mesenchymal progenitor cells. *Arthritis Rheum.* **2002**, *46*, 3349–3360. [[CrossRef](#)]
34. Jones, E.A.; English, A.; Henshaw, K.; Kinsey, S.E.; Markham, A.F.; Emery, P.; McGonagle, D. Enumeration and phenotypic characterization of synovial fluid multipotential mesenchymal progenitor cells in inflammatory and degenerative arthritis. *Arthritis Rheum.* **2004**, *50*, 817–827. [[CrossRef](#)]
35. Ghaben, A.L.; Scherer, P.E. Adipogenesis and metabolic health. *Nat. Rev. Mol. Cell Biol.* **2019**, *20*, 242–258. [[CrossRef](#)] [[PubMed](#)]
36. Russell, T.; Watad, A.; Bridgewood, C.; Rowe, H.; Khan, A.; Rao, A.; Loughenbury, P.; Millner, P.; Dunsmuir, R.; Cuthbert, R.; et al. Il-17a and tnf modulate normal human spinal enthesal bone and soft tissue mesenchymal stem cell osteogenesis, adipogenesis, and stromal function. *Cells* **2021**, *10*, 341. [[CrossRef](#)]
37. Deng, J.; Hua, K.; Lesser, S.S.; Harp, J.B. Activation of signal transducer and activator of transcription-3 during proliferative phases of 3t3-l1 adipogenesis. *Endocrinology* **2000**, *141*, 2370–2376. [[CrossRef](#)]
38. Floyd, Z.E.; Stephens, J.M. Stat5a promotes adipogenesis in nonprecursor cells and associates with the glucocorticoid receptor during adipocyte differentiation. *Diabetes* **2003**, *52*, 308–314. [[CrossRef](#)]
39. Zhang, K.; Guo, W.; Yang, Y.; Wu, J. Jak2/stat3 pathway is involved in the early stage of adipogenesis through regulating c/ebp β transcription. *J. Cell. Biochem.* **2011**, *112*, 488–497. [[CrossRef](#)]
40. Nanbu-Wakao, R.; Morikawa, Y.; Matsumura, I.; Masuho, Y.; Muramatsu, M.A.; Senba, E.; Wakao, H. Stimulation of 3t3-l1 adipogenesis by signal transducer and activator of transcription 5. *Mol. Endocrinol.* **2002**, *16*, 1565–1576. [[CrossRef](#)]
41. Lowe, C.E.; O’Rahilly, S.; Rochford, J.J. Adipogenesis at a glance. *J. Cell Sci.* **2011**, *124*, 2681–2686. [[CrossRef](#)]
42. Gregoire, F.; De Broux, N.; Hauser, N.; Heremans, H.; Van Damme, J.; Remacle, C. Interferon-gamma and interleukin-1 beta inhibit adipoconversion in cultured rodent preadipocytes. *J. Cell. Physiol.* **1992**, *151*, 300–309. [[CrossRef](#)]
43. Song, H.Y.; Jeon, E.S.; Kim, J.I.; Jung, J.S.; Kim, J.H. Oncostatin m promotes osteogenesis and suppresses adipogenic differentiation of human adipose tissue-derived mesenchymal stem cells. *J. Cell. Biochem.* **2007**, *101*, 1238–1251. [[CrossRef](#)]
44. White, U.A.; Stewart, W.C.; Mynatt, R.L.; Stephens, J.M. Neuropoietin attenuates adipogenesis and induces insulin resistance in adipocytes. *J. Biol. Chem.* **2008**, *283*, 22505–22512. [[CrossRef](#)] [[PubMed](#)]
45. Yue, R.; Zhou, B.O.; Shimada, I.S.; Zhao, Z.; Morrison, S.J. Leptin receptor promotes adipogenesis and reduces osteogenesis by regulating mesenchymal stromal cells in adult bone marrow. *Cell Stem Cell* **2016**, *18*, 782–796. [[CrossRef](#)]
46. Zhou, B.O.; Yue, R.; Murphy, M.M.; Peyer, J.G.; Morrison, S.J. Leptin-receptor-expressing mesenchymal stromal cells represent the main source of bone formed by adult bone marrow. *Cell Stem Cell* **2014**, *15*, 154–168. [[CrossRef](#)]
47. Cernkovich, E.R.; Deng, J.; Bond, M.C.; Combs, T.P.; Harp, J.B. Adipose-specific disruption of signal transducer and activator of transcription 3 increases body weight and adiposity. *Endocrinology* **2008**, *149*, 1581–1590. [[CrossRef](#)]
48. Shi, S.Y.; Luk, C.T.; Brunt, J.J.; Sivasubramaniyam, T.; Lu, S.Y.; Schroer, S.A.; Woo, M. Adipocyte-specific deficiency of janus kinase (jak) 2 in mice impairs lipolysis and increases body weight, and leads to insulin resistance with ageing. *Diabetologia* **2014**, *57*, 1016–1026. [[CrossRef](#)]
49. Stechschulte, L.A.; Lecka-Czernik, B. Reciprocal regulation of ppar γ and runx2 activities in marrow mesenchymal stem cells: Fine balance between p38 mapk and protein phosphatase 5. *Curr. Mol. Biol. Rep.* **2017**, *3*, 107–113. [[CrossRef](#)]

50. Rauch, A.; Haakonsson, A.K.; Madsen, J.G.S.; Larsen, M.; Forss, I.; Madsen, M.R.; Van Hauwaert, E.L.; Wiwie, C.; Jespersen, N.Z.; Tencerova, M.; et al. Osteogenesis depends on commissioning of a network of stem cell transcription factors that act as repressors of adipogenesis. *Nat. Genet.* **2019**, *51*, 716–727. [[CrossRef](#)]
51. Krueger, J.; Clark, J.D.; Suárez-Fariñas, M.; Fuentes-Duculan, J.; Cueto, I.; Wang, C.Q.; Tan, H.; Wolk, R.; Rottinghaus, S.T.; Whitley, M.Z.; et al. Tofacitinib attenuates pathologic immune pathways in patients with psoriasis: A randomized phase 2 study. *J. Allergy Clin. Immunol.* **2016**, *137*, 1079–1090. [[CrossRef](#)]
52. Sherlock, J.P.; Joyce-Shaikh, B.; Turner, S.P.; Chao, C.C.; Sathe, M.; Grein, J.; Gorman, D.M.; Bowman, E.P.; McClanahan, T.K.; Yearley, J.H.; et al. Il-23 induces spondyloarthritis by acting on ror-gammat+ cd3+cd4-cd8- enthesal resident t cells. *Nat. Med.* **2012**, *18*, 1069–1076. [[CrossRef](#)]
53. Lubrano, E.; Massimo Perrotta, F.; Manara, M.; D'Angelo, S.; Addimanda, O.; Ramonda, R.; Punzi, L.; Olivieri, I.; Salvarani, C.; Marchesoni, A. Predictors of loss of remission and disease flares in patients with axial spondyloarthritis receiving antitumor necrosis factor treatment: A retrospective study. *J. Rheumatol.* **2016**, *43*, 1541–1546. [[CrossRef](#)]
54. Jacques, P.; Lambrecht, S.; Verheugen, E.; Pauwels, E.; Kollias, G.; Armaka, M.; Verhoye, M.; Van der Linden, A.; Achten, R.; Lories, R.J. Proof of concept: Enthesitis and new bone formation in spondyloarthritis are driven by mechanical strain and stromal cells. *Ann. Rheum. Dis.* **2014**, *73*, 437–445. [[CrossRef](#)]
55. Reinhardt, A.; Yevsa, T.; Worbs, T.; Lienenklaus, S.; Sandrock, I.; Oberdörfer, L.; Korn, T.; Weiss, S.; Förster, R.; Prinz, I. Interleukin-23-dependent γ/δ t cells produce interleukin-17 and accumulate in the enthesitis, aortic valve, and ciliary body in mice. *Arthritis Rheumatol.* **2016**, *68*, 2476–2486. [[CrossRef](#)]
56. Godfrey, D.I.; Uldrich, A.P.; McCluskey, J.; Rossjohn, J.; Moody, D.B. The burgeoning family of unconventional t cells. *Nat. Immunol.* **2015**, *16*, 1114–1123. [[CrossRef](#)]
57. Cole, S.; Murray, J.; Simpson, C.; Okoye, R.; Tyson, K.; Griffiths, M.; Baeten, D.; Shaw, S.; Maroof, A. Interleukin (il)-12 and il-18 synergize to promote mait cell il-17a and il-17f production independently of il-23 signaling. *Front. Immunol.* **2020**, *11*, 2992. [[CrossRef](#)]
58. Lee, J.S.; Tato, C.M.; Joyce-Shaikh, B.; Gulen, M.F.; Cayatte, C.; Chen, Y.; Blumenschein, W.M.; Judo, M.; Ayanoglu, G.; McClanahan, T.K. Interleukin-23-independent il-17 production regulates intestinal epithelial permeability. *Immunity* **2015**, *43*, 727–738. [[CrossRef](#)]
59. Sakaguchi, N.; Takahashi, T.; Hata, H.; Nomura, T.; Tagami, T.; Yamazaki, S.; Sakihama, T.; Matsutani, T.; Negishi, I.; Nakatsuru, S.; et al. Altered thymic t-cell selection due to a mutation of the zap-70 gene causes autoimmune arthritis in mice. *Nature* **2003**, *426*, 454–460. [[CrossRef](#)] [[PubMed](#)]
60. Oh, K.; Seo, M.W.; Kim, I.G.; Hwang, Y.I.; Lee, H.Y.; Lee, D.S. Cp-690550 treatment ameliorates established disease and provides long-term therapeutic effects in an skg arthritis model. *Immune Netw.* **2013**, *13*, 257–263. [[CrossRef](#)]
61. Sendo, S.; Saegusa, J.; Yamada, H.; Nishimura, K.; Morinobu, A. Tofacitinib facilitates the expansion of myeloid-derived suppressor cells and ameliorates interstitial lung disease in skg mice. *Arthritis Res. Ther.* **2019**, *21*, 184. [[CrossRef](#)]
62. Gracey, E.; Hromadová, D.; Lim, M.; Qaiyum, Z.; Zeng, M.; Yao, Y.; Srinath, A.; Baglaenko, Y.; Yeremenko, N.; Westlin, W. Tyk2 inhibition reduces type 3 immunity and modifies disease progression in murine spondyloarthritis. *J. Clin. Investig.* **2020**, *130*, 1863–1878. [[CrossRef](#)]
63. Meissburger, B.; Ukropec, J.; Roeder, E.; Beaton, N.; Geiger, M.; Teupser, D.; Civan, B.; Langhans, W.; Nawroth, P.P.; Gasperikova, D.; et al. Adipogenesis and insulin sensitivity in obesity are regulated by retinoid-related orphan receptor gamma. *EMBO Mol. Med.* **2011**, *3*, 637–651. [[CrossRef](#)]
64. Jetten, A.M. Retinoid-related orphan receptors (rors): Critical roles in development, immunity, circadian rhythm, and cellular metabolism. *Nucl. Recept. Signal.* **2009**, *7*, e003. [[CrossRef](#)]